Libyan Journal of Sustainable Development Research
المجلة الليبية لأبحاث التنمية المستدامة
E-ISSN: 3136-313X
Volume 2, Issue 2, 2026
Page No: 84-96
Website: https://ljsdr.ly/index.php/ljsdr/index

Experimental Investigation of Current, Voltage, and Operating Temperature Effects on Solar-Powered Green Hydrogen Production

Yuosef Adraider[1], Ibrahim Imbayah[2], Ali Elhatmi[3], Mohamed Aboseif[4], Shima Althabet[5], Yousuf Emran[6], Elmahboub Edreder[7]

[1,2,3,4,5,6]Department of Energy Engineering, College of Renewable Energy, Tajoura, Libya

[7]Petrochemicals and Gas Division, National Oil Corporation, Libya

دراسة تجريبية لتأثير التيار والجهد ودرجة حرارة التشغيل في إنتاج الهيدروجين الأخضر باستخدام الطاقة الشمسية

يوسف أدرايدر[1]، إبراهيم إمبيه[2]، علي الحاتمي[3]، محمد أبوسيف[4]، شيما الثابت[5]، يوسف عمران[6]، المحبوب إدريدير[7]

[1,2,3,4,5,6]قسم هندسة الطاقة، كلية الطاقة المتجددة، تاجوراء، ليبيا

[7]قسم البتروكيماويات والغاز، المؤسسة الوطنية للنفط ، ليبيا

*Corresponding author: ibrahim.alzayani@gmail.com

Received: May 02, 2026	Revised: July 06, 2026	Accepted: July 22, 2026
	Published: July 30, 2026	

Abstract:
The study was conducted within the global transition toward sustainable energy systems and the reduction of carbon emissions, where green hydrogen has emerged as a key clean energy carrier capable of storing energy. The main objective of this study is to investigate the performance of a small-scale green hydrogen production system powered by solar energy, with particular emphasis on the influence of operating parameters on hydrogen energy production. The integrated system was designed and implemented, utilizing photovoltaic (PV) panels to power a Proton Exchange Membrane (PEM) electrolyzer. A block diagram was developed to illustrate the interconnected system components. The methodology encompassed operating the system and conducting empirical experiments under varying operational conditions by adjusting the voltage, electrical current, and temperature, alongside recording and analyzing the fundamental operational data. At an operational current of about 7.0 A and voltage of about 1.82 V, the system produced a steady-state hydrogen flow rate of around 48 mL/min. In comparison to steam methane reforming, the pilot system might reduce CO_2 emissions by 9–12 kg CO_2 per kg of green hydrogen produced, with an estimated LCOH of \$8.5–11.2/kg H_2. Ohmic-dominated behavior throughout the measured range was confirmed by the voltage–current relationship's linear correlation ($R^2 > 0.99$). The results revealed a direct correlation between the operational variables and the green hydrogen production rate, where an increase in electrical current yielded higher production. Furthermore, precise control of voltage and temperature contributed to optimizing the process efficiency. This makes the proposed system an effective step toward green hydrogen production, demonstrating promising potential for further development and integration with renewable energy sources in future applications.

Keywords: Green hydrogen, Renewable energy, Electrolyzer, Low carbon emissions.

الملخص:
أُجريت هذه الدراسة في سياق التحول العالمي نحو أنظمة الطاقة المستدامة وخفض انبعاثات الكربون، حيث برز الهيدروجين الأخضر كناقل رئيسي للطاقة النظيفة قادر على تخزين الطاقة. ويتمثل الهدف الرئيسي لهذه الدراسة في تقييم أداء نظام صغير الحجم لإنتاج الهيدروجين الأخضر يعمل بالطاقة الشمسية، مع التركيز بشكل خاص على تأثير معلمات التشغيل على إنتاج طاقة الهيدروجين. تم تصميم وتنفيذ النظام المتكامل باستخدام الألواح الكهروضوئية (PV) لتشغيل جهاز التحليل الكهربائي بغشاء تبادل البروتونات (PEM). كما تم وضع مخطط تخطيطي لتوضيح مكونات النظام المترابطة. وشملت المنهجية تشغيل النظام وإجراء تجارب تجريبية في ظل ظروف تشغيلية متنوعة من خلال تعديل الجهد الكهربائي والتيار الكهربائي ودرجة الحرارة، إلى جانب تسجيل البيانات التشغيلية الأساسية وتحليلها. عند تيار تشغيلي يبلغ حوالي 7.0 أمبير وجهد يبلغ حوالي 1.82 فولت، أنتج النظام معدل تدفق هيدروجين في حالة مستقرة يبلغ حوالي 48 مل/دقيقة. وبالمقارنة مع عملية إعادة تشكيل الميثان بالبخار، قد يقلل النظام التجريبي من انبعاثات ثاني أكسيد الكربون بمقدار 9–12 كجم من ثاني أكسيد الكربون لكل كيلوغرام من الهيدروجين الأخضر المنتج، مع تكلفة هيدروجين منخفضة (LCOH) تقدر بـ 8.5–11.2 دولار/كجم H2. تم تأكيد السلوك الذي يهيمن عليه المقاومة الأومية عبر النطاق المقاس من خلال الارتباط الخطي لعلاقة الجهد بالتيار ($R^2 > 0.99$). وكشفت النتائج عن وجود ارتباط مباشر بين المتغيرات التشغيلية ومعدل إنتاج الهيدروجين الأخضر، حيث أدت الزيادة في التيار الكهربائي إلى ارتفاع الإنتاج. علاوة على ذلك، ساهم التحكم الدقيق في الجهد والحرارة في تحسين كفاءة العملية. وهذا يجعل النظام المقترح خطوة فعالة نحو إنتاج الهيدروجين الأخضر، مما يظهر إمكانات واعدة لمزيد من التطوير والتكامل مع مصادر الطاقة المتجددة في التطبيقات المستقبلية.

الكلمات المفتاحية: الهيدروجين الأخضر، الطاقة المتجددة، محلل كهربائي، انبعاثات الكربون المنخفضة.

1. Introduction

The increasing potential of hybrid renewable energy systems for low-carbon energy applications and sustainable hydrogen production has been shown by recent studies [1-3]. The technological viability and environmental advantages of integrated grid-wind-hydrogen systems, which may provide power, freshwater, and hydrogen fuel all at once, have been studied by several researchers in areas with significant potential for renewable energy. Incorporating electrolysis with renewable energy can greatly lower greenhouse gas emissions while enhancing energy security [4,5], according to other research that assessed photovoltaic-powered hydrogen systems for urban electricity delivery [6-9]. To improve renewable energy consumption, optimize operating costs, and increase system reliability, multi-source hybrid renewable energy systems that include solar, wind, biomass, battery storage, and hydrogen technologies have also been proposed [10-13].

Furthermore, recent studies on photovoltaic-battery-diesel hybrid systems have shown practical methods for reducing the cost of producing hydrogen while preserving dependable system performance in the face of fluctuating renewable energy conditions [14-17]. The strategic role of renewable hydrogen in attaining energy sustainability, lowering reliance on fossil fuels, and supporting national decarbonization goals has been further highlighted by additional regional studies that focus on green hydrogen production for sustainable transportation, hydrogen-sector investment planning, and wind-powered hydrogen generation [18-22]. The significance of the current work in promoting economically feasible and ecologically sustainable green hydrogen production is reinforced by these recent contributions, which offer useful benchmarks for assessing renewable hydrogen systems [23-27].

Over the past decades, carbon emissions have massively increased due to many factors, such as the increase in population, electricity generation, manufacturing processes, and transportation [28-35]. Fossil fuels continue to dominate the global energy consumption landscape, accounting for the largest share of global energy consumption [36-40]. According to the International Energy Agency, fossil fuel consumption in 2023 accounted for approximately 81% of total global primary energy consumption, a slight decrease from previous years, but still a significant majority [41-43].

This continued reliance on carbon-intensive energy sources poses serious environmental risks, such as increased air pollution, accelerated habitat degradation, and more frequent extreme weather events due to climate change [44-48]. If no action is taken, the global temperature rise could exceed critical thresholds, potentially leading to irreversible climate change and devastating impacts on ecosystems, human health, and the economy [49-53].

In response to these challenges, the international community is accelerating the pace of transformation in the energy sector by moving from fossil fuel-based energy production and consumption systems – including oil, natural gas, and coal – to renewable energy sources such as wind, solar, and hydroelectric power. The International Renewable Energy Agency (IRENA) projects that the share of renewable energy in the global energy mix will rise from 16% in 2020 to 77% by 2050, based on a 1.5°C temperature increase scenario [54-56].

By 2050, hydrogen produced from renewable sources and low-carbon technologies is expected to account for between 73% and 100% of total global hydrogen demand [57-60]. Hydrogen is expected to play a crucial role in reducing carbon emissions in end-use sectors and enhancing the resilience of the energy system. The produced hydrogen is mostly used in many industrial applications, such as fertilizers, petroleum refining processes, petrochemicals, fuel cells, and chemical industries. Hydrogen can be produced through several routes, including steam methane reforming, coal gasification, and water electrolysis [61-64]. The common technologies of hydrogen production are summarized in Figure. 1. It is noted that hydrogen production depends on many key factors such as efficiency, cost-effective electrocatalysts, and durability.

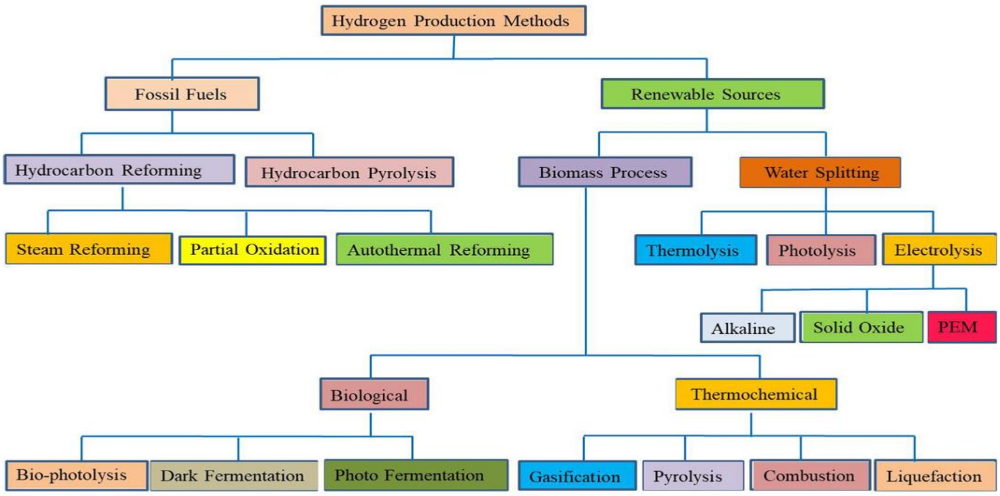

Figure 1. Hydrogen Production Technologies.

The integration of renewable energy sources with hydrogen production provides a promising future due to zero–carbon emissions in the long term, providing many advantages such as low-cost electrocatalysts, high efficiency, and the possibility for reduction of energy consumption [65]. This study investigates the impact of operational variables on a small-scale pilot system for producing green hydrogen using solar energy. It includes developing a block diagram illustrating the interrelationships of the system's components. The study also involves conducting practical experiments and measurements to examine the effect of operational variables such as voltage, current, and temperature on the amount of green hydrogen produced. Furthermore, it includes recording and analyzing the system's basic operational data during operation. Finally, the study analyzes the impact of voltage and current data, extracts operational curves, and calculates the green hydrogen production rate to determine the system's optimal performance [66-70].

The deployment of renewable energy has grown at an unprecedented rate globally due to growing worries about climate change, energy security, and the pressing need to cut greenhouse gas emissions. The installed renewable energy capacity in the world grew by around 50% to almost 4,448.1 GW in 2024. In the worldwide energy transition, solar photovoltaic (PV) technology accounted for around 2,200 GW, while wind power contributed about 1,021 GW. Green hydrogen technologies have advanced remarkably at the same time, with an installed electrolysis capacity of about 5 GW worldwide. Additionally, the total installed capacity of battery energy storage systems (BESS) increased to around 150 GW (363 GWh), offering crucial dependability and flexibility for incorporating variable renewable energy sources into contemporary power systems [71-76]. Above-mentioned advancements highlight the growing significance of hydrogen generation powered by renewable energy as a crucial route for accomplishing long-term decarbonization objectives and show how quickly the world is moving toward sustainable and low-carbon energy systems.

2. Experimental Procedure

The methodology employed in this study relies on the implementation and assembly of a miniaturized system for producing green hydrogen using photovoltaic solar energy, with a focus on the system's practical and engineering aspects. The process moves from basic concepts to an operational and testable integrated system, thus achieving the project's research objectives. The proposed system represents a miniature experimental model for the production of green hydrogen using photovoltaic solar energy. It has been implemented to operate as an independent and controllable system for research and laboratory study purposes. The system relies on integrating solar energy generation technologies with water electrolysis to produce hydrogen without carbon emissions.

The block diagram of the system represents the general geometric representation of the connection of the different components and illustrates the paths of energy and material flow within the system. It is an essential tool for understanding the operational structure of the system and how it works as a whole. The block diagram of the system is shown in Figure 2, illustrating the functional relationship between the different subsystems and the sequence of transfer of electrical energy, water, and gases from the moment of generation until the production of green hydrogen.

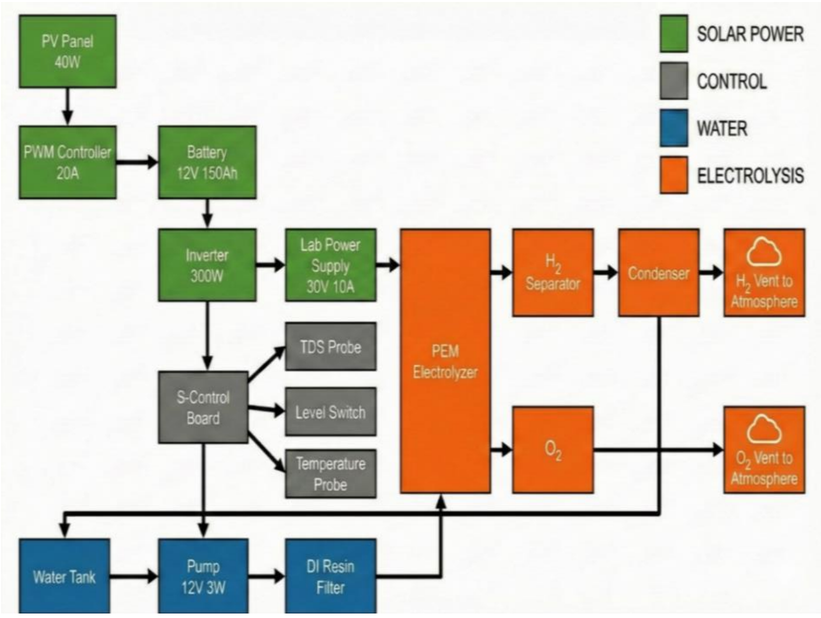

Figure. 2. Block Diagram of Experiment.

The system consists of a set of main subsystems that work in an integrated manner with each other, including the electrical supply and power conditioning system, the water treatment and electrolyzer supply system, the electrolysis and gas separation unit, in addition to the control and monitoring system. This integration enables stable and safe operation of the system, with the ability to monitor and control operating variables during experiments. The experimental photo including tools and devices is shown in Figure. 3.

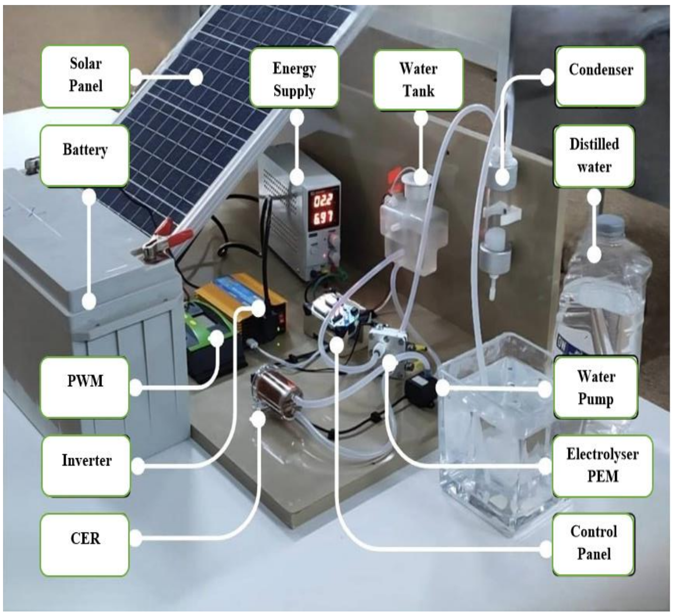

Figure 3. Experimental Photo.

3. Results and Discussion

Mathematical Modeling of the System Components

The main components of the suggested renewable energy system were described mathematically to give a thorough explanation. The theoretical foundation for the simulation and performance assessment is provided by these models.

Photovoltaic Array Model

The operational cell temperature and incident solar irradiation have an impact on the ph:

$$V_{PV} = V_{STC}[1 + \beta_V(T_{cell} - T_{STC})] + ln\frac{H_t}{H_{STC}} \quad (1)$$

$$I_{PV} = I_{STC}[1 + \beta_I(T_{cell} - T_{STC})]\frac{H_t}{H_{STC}} \quad (2)$$

Where: T_{STC} and T_{cell} are the cell's surface temperature at Standard Test Condition and under real operation conditions (°C), β_V and β_I are the Voltage and Current temperature coefficients (%/°C), and H_{STC} and H_t are the STC and real global solar irradiance incident on the PV module surface. The challenge that researchers will face is to find an empirical equation to determine the cell surface temperature. T_{cell} For example:

$$T_{cell} = T_{\infty} + 7.8 \times 10^{-2}H_t \quad (3)$$

Photovoltaic array's output voltage and current [29, 30]. They are expressed as.

Battery modeling

$$SoC(t) = SoC(t-1).(1-\sigma) + \left(\mathrm{P}_{sys}(\mathrm{t}) - \frac{P_L(t)}{\eta_{inv}}\right) \times \eta_b \quad (4)$$

Battery capacity:

$$P_B = \frac{\max[SoC(t)]_{t=1,8760}}{DOD} \times \mathrm{CF}_T \quad (5)$$

Temperature correction factor:

$$\mathrm{CF}_T = 0.0004T^2 - 0.0246T + 1.3961 \quad (6)$$

Electrolyzer and fuel cell may be estimated:

$$\dot{m}_{H_2}(t) = \left[\frac{P \times \eta_{El}}{LHV_{H_2}}\right] \quad (7)$$

Where, $\dot{m}_{H_2}(t)$ is the H_2 productivity (ton/hr) powered P (MW), LHV_{H_2} is the lower heating value of H_2 (33.3 $kWh/kg\ H_2$) and η_{El} is the electrolyzer efficiency (80%) [31].

Fuel cell P_{FC} (MW) is determined as:

$$P_{FC}(t) = [\dot{m}_{H_2}(t) \times LHV_{H_2} \times \eta_{FC}] \quad (8)$$

Where: η_{FC} represents the fuel cell efficiency (60%).

Full Electrical and Thermal Characteristics

Providing the complete manufacturer-rated electrical and thermal parameters under Standard Test Conditions (STC: 1000 W/m², cell temperature 25 °C, AM 1.5) and Nominal Operating Cell Temperature (NOCT) conditions shown in Table 1.

Table 1. Electrical and thermal characteristics of the 40 Wp polycrystalline silicon PV module.

Parameter	Symbol	Value at STC	Value at NOCT
Maximum Power	P_{max}	40 W	~30 W
Maximum Power Voltage	V_{mp}	18.2 V	~16.5 V
Maximum Power Current	I_{mp}	2.20 A	~1.82 A
Open-Circuit Voltage	V_{oc}	22.2 V	~20.5 V
Short-Circuit Current	I_{sc}	2.37 A	~1.96 A
Module Efficiency	η_{module}	~12.8 %	-
Temperature Coefficient of Power	γ_P	−0.47 %/°C	-
Temperature Coefficient of Voltage	β_V	−0.34 %/°C	-
Temperature Coefficient of Current	β_I	+0.06 %/°C	-
Nominal Operating Cell Temperature	*NOCT*	-	45 ± 2 °C
Operating Temperature Range	-	−40 °C to +85 °C	-
Maximum System Voltage	$V_{sys,\ max}$	1000 V DC	-

The variation of current (A) as a function of time (min) over a 10-minute interval is shown in Figure 4. The current displays a slight decreasing trend with minor fluctuations, indicating a relatively stable system with small transient changes. The current is at its maximum value of approximately 6.990 A at the first minute (1 min). A noticeable drop occurs between 1 and 2 minutes, where the current decreases to around 6.973 A. From 2 to 5 minutes, the current stabilizes, fluctuating narrowly around 6.973–6.970 A, suggesting a quasi-steady-state condition. Between 5 and 7 minutes, a gradual decline is observed, reaching about 6.963 A at 7 minutes.

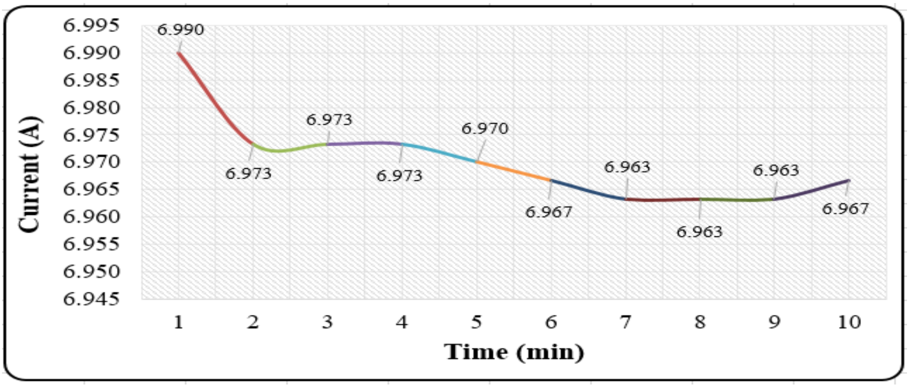

Figure 4. Current vs Time.

This indicates a slow reduction in current, possibly due to system equilibration, temperature effects, or minor resistance changes. From 7 to 9 minutes, the current remains nearly constant at approximately 6.963 A, reinforcing the presence of a stable operating regime. A slight increase is seen at 10 minutes (≈6.967 A), which may reflect minor recovery or measurement variation. The data demonstrate an initial transient decrease followed by a stable operating system with minimal fluctuations (within ~0.03 A). This behavior suggests that the system quickly reaches equilibrium and maintains consistent performance over time, with only negligible drift.

The temporal evolution of voltage (V) over 10 minutes is displayed in Figure 5. The voltage profile shows an initial rise followed by a stable plateau, indicating that the system rapidly reaches and maintains a steady operating condition. At the start of the measurement (1 min), the voltage is approximately 1.8187 V. A gradual increase is observed between 1 and 2 minutes, reaching about 1.8193 V. This is followed by a more pronounced rise between 2 and 3 minutes, where the voltage attains ~1.8213 V.

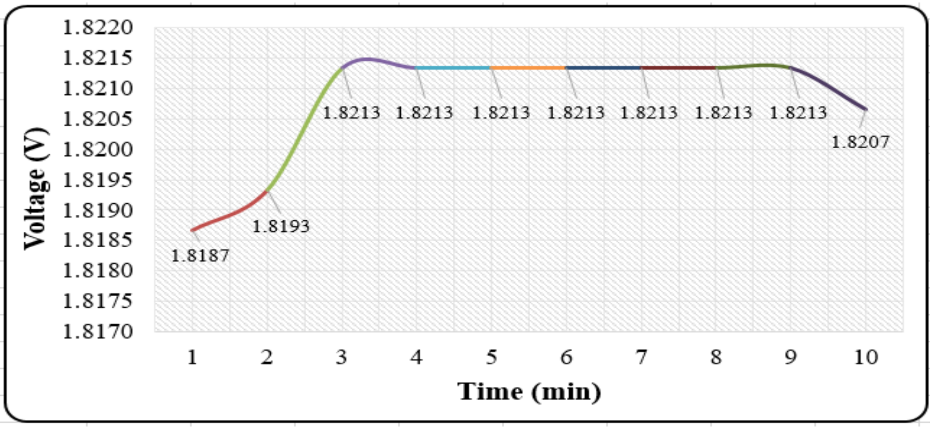

Figure 5. Voltage vs Time.

This sharp increase suggests a transient response phase, likely associated with system activation, stabilization of electrochemical processes, or equilibration effects. From 3 to 9 minutes, the voltage remains nearly constant at approximately 1.8213 V, with negligible fluctuations. This extended plateau indicates a highly stable steady-state regime, reflecting consistent system performance and minimal internal variation over time. At 10 minutes, a slight decrease to around 1.8207 V is observed. This minor drop may be attributed to small changes in operating conditions, such as temperature variation, slight polarization effects, or measurement uncertainty. The voltage variation is very small (within ~0.003 V), demonstrating excellent stability after the initial transient phase. The results confirm that the system achieves steady-state operation quickly and maintains a consistent voltage output over the duration of the experiment.

The relationship between voltage (V) and current (A) is depicted in Figure 6, showing a clear positive correlation across the measured range. As the current increases from approximately 3.5 A to 8 A, the voltage rises steadily from about 1.688 V to 1.871 V.

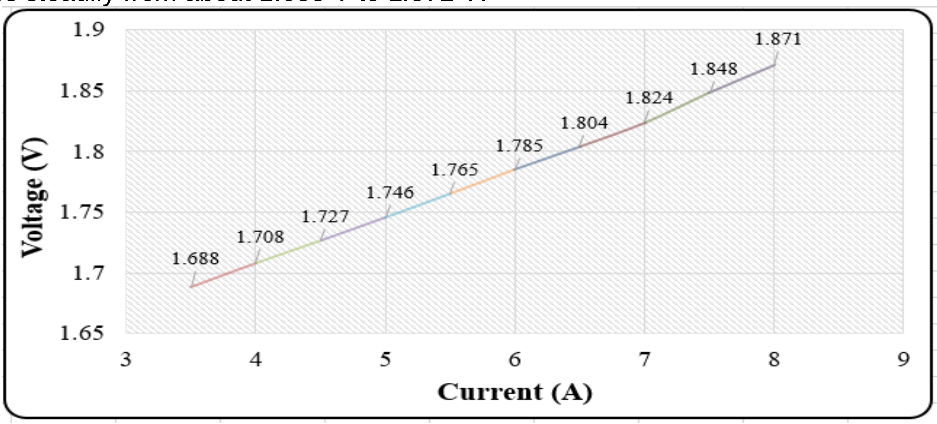

Figure 6. Voltage vs Current.

The trend is nearly linear, indicating that the system follows a predictable voltage–current behavior over the tested operating region. At lower currents (~3.5–4.5 A), the voltage increases gradually from 1.688 V to 1.727 V. As the current continues to rise, the voltage exhibits a consistent incremental increase: reaching 1.746 V at ~5 A, 1.785 V at ~6 A, and 1.824 V at ~7 A. At higher currents (~7.5–8 A), the voltage further increases to 1.848 V and finally 1.871 V. The absence of significant deviations or curvature suggests minimal nonlinear effects within this range, implying stable internal resistance and uniform system behavior.

The slope of the curve reflects the effective resistance or polarization characteristics of the system, with the linearity indicating that resistive losses dominate over other complex mechanisms. The results demonstrate a stable and proportional voltage response to increasing current, which is characteristic of a well-behaved system operating within its normal regime. This linear trend also supports the reliability and reproducibility of the measurements.

The variation of cell temperature (°C) as a function of time (minutes) over 10 minutes is shown in Figure 7. The temperature exhibits a gradual increasing trend, rising from approximately 19.3 °C at the start to about 19.7 °C by the end of the observation period. In the initial phase (1–3 minutes), the temperature remains relatively stable with only a slight increase from 19.3 °C to 19.3–19.4 °C, indicating a near steady-state condition. Between 3 and 6 minutes, a more noticeable rise occurs, with the temperature reaching around 19.5 °C. A brief plateau is observed around 6–7 minutes, where the temperature stabilizes at approximately 19.5 °C, suggesting a temporary balance between heat generation and dissipation.

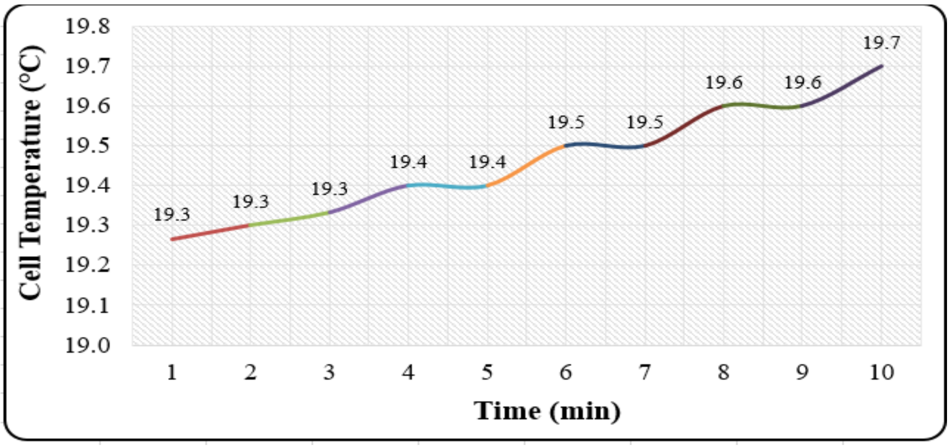

Figure. 7. Cell Temperature vs Time.

From 7 to 10 minutes, the temperature resumes its upward trend, increasing steadily to 19.7 °C. This final phase indicates continued heat accumulation within the system. Despite minor fluctuations, the overall behavior is characterized by a consistent and controlled temperature rise, with no abrupt changes or instability. This trend suggests that the system undergoes gradual thermal buildup over time, likely due to sustained operation or continuous energy input, while maintaining relatively stable thermal dynamics throughout the experiment.

The variation of hydrogen flow rate (mL/min) as a function of time over a 10-minute interval is shown in Figure 8. Unlike the temperature profile, the hydrogen flow exhibits a fluctuating pattern, indicating dynamic system behavior. At the beginning (1–2 minutes), the flow rate increases from approximately 47 mL/min to 48 mL/min. A slight dip follows at 3 minutes, though the value remains close to 48 mL/min. The flow then rises to a local maximum of about 49 mL/min at 4 minutes, representing the peak value observed during the experiment. Between 4 and 6 minutes, the flow rate decreases to around 47.5 mL/min before increasing again to approximately 48.5 mL/min at 6 minutes, suggesting short-term oscillatory behavior. After this point, a more pronounced decline occurs, reaching a minimum of about 46.5 mL/min at 8 minutes.

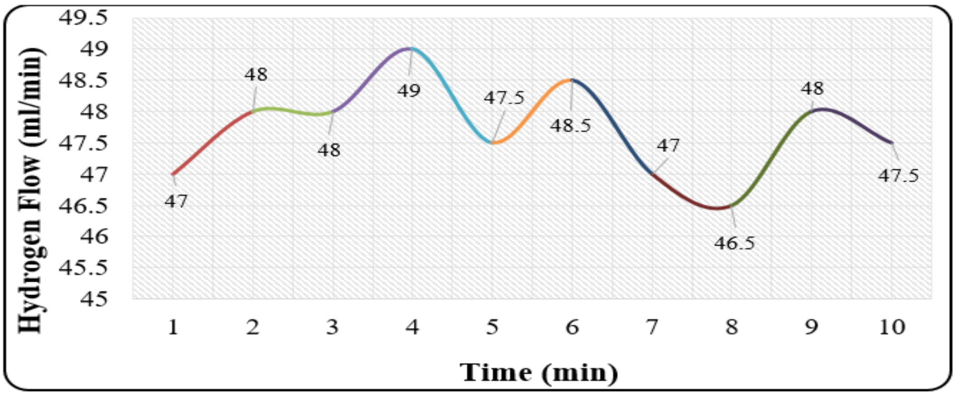

Figure. 8. Hydrogen Flow rate vs time.

In the final phase (8–10 minutes), the hydrogen flow recovers to approximately 48 mL/min at 9 minutes, followed by a slight decrease to 47.5 mL/min at 10 minutes. Overall, the profile demonstrates periodic fluctuations around an average value near 48 mL/min, without a clear long-term increasing or decreasing trend. These variations likely reflect transient changes in system conditions, such as pressure, reaction kinetics, or flow regulation mechanisms, while maintaining overall operational stability within a relatively narrow range.

4. Assumptions, Limitations, and Uncertainties

Assumptions:

1. The electrolyzer operates under steady-state conditions after an initial transient period (~3 minutes);
2. The PEM membrane maintains constant ionic conductivity throughout the experiment;
3. Water purity remains constant (deionized water, resistivity > 18 MΩ·cm);
4. Ambient pressure is constant at 1 atm;
5. Gas collection is performed at standard temperature and pressure (STP) conditions;
6. The PV panel output is treated as a DC power source with negligible ripple.

Limitations:

1. The study is limited to a small-scale laboratory system (40 W PV panel);
2. Experiments were conducted under controlled indoor conditions, not real outdoor solar irradiance;
3. The observation period (10 minutes per trial) may not capture long-term degradation effects;
4. Only one type of PEM electrolyzer was tested;
5. The temperature range was limited (19.3–19.7 °C), restricting the generalizability of thermal effects.

Uncertainties:

1. Current measurement uncertainty: ±0.005 A (digital multimeter accuracy);
2. Voltage measurement uncertainty: ±0.001 V;
3. Temperature measurement uncertainty: ±0.1 °C (thermocouple accuracy);
4. Hydrogen flow rate measurement uncertainty: ±0.5 mL/min (graduated cylinder/sensor resolution);
5. Combined expanded uncertainty in hydrogen production rate: approximately ±2.5% (at 95% confidence level).

5. Conclusion

The experimental results reveal that the system achieves rapid stabilization and maintains highly consistent performance throughout the 10-minute operation period. The current profile shows a slight initial decrease followed by a stable plateau with minimal fluctuations, indicating quick attainment of electrical steady-state conditions. Similarly, the voltage exhibits a short transient rise before stabilizing within a very narrow range, confirming reliable and stable electrochemical behavior. The voltage–current relationship reveals a clear linear correlation, suggesting that the system operates within a predictable regime dominated by ohmic characteristics, with negligible nonlinear or polarization effects. This linearity reflects stable internal resistance and supports the reliability of the measurements.

Thermally, the gradual increase in cell temperature indicates controlled heat accumulation without instability, implying effective thermal management during operation. In contrast, the hydrogen flow rate displays minor oscillations around a constant average, highlighting dynamic but well-regulated flow behavior likely influenced by transient system adjustments. These results confirm that the system operates under stable, well-controlled conditions with minimal drift in key parameters (current, voltage, temperature, and hydrogen flow). The rapid transition to steady-state operation, combined with consistent performance and linear electrical characteristics, demonstrates the robustness, reliability, and reproducibility of the system within the investigated operating range.

Funding: This research received no external funding.

Acknowledgments: The authors would like to express their sincere appreciation to the Libyan Center for Sustainable Development Research, Al-Khums, Libya, for its valuable academic support and institutional facilitation that contributed to the completion and publication of this article.

Conflicts of Interest: The authors declare no conflicts of interest.

References

[1] A. Karabuga, E. Cuce, P. M. Cuce, and Z. Utlu, "Comparative performance and economic analysis for different clean energy and hydrogen production systems: A case study for Türkiye," *Int. J. Hydrogen Energy*, vol. 201, no. 152933, p. 152933, 2026.

[2] Z. Wang *et al.*, "Efficient low-carbon hydrogen production driven by solar energy: Properties, challenges and future perspectives," *Fuel (Lond.)*, vol. 407, no. 137500, p. 137500, 2026.

[3] M. Khaleel, Z. Yusupov, M. Guneser, H. El-Khozondar, A. Ahmed, and A. A. Alsharif, "Towards hydrogen sector investments for achieving sustainable electricity generation," *jsesd*, vol. 13, no. 1, pp. 71–96, 2024.

[4] S. Goel and R. Sharma, “Green hydrogen production from hybrid renewable energy systems: a techno-economic analysis in Rural India,” *Int. J. Sustain. Energy*, vol. 45, no. 1, 2026.
[5] M. Khaleel, Z. Yusupov, and S. Rekik, “Advancing hydrogen as a key driver for decarbonized power systems,” *Unconventional Resources*, vol. 9, no. 100278, p. 100278, 2026.
[6] H. J. El-Khozondar *et al.*, “Analysis of a grid/wind/hydrogen hybrid energy system for producing electricity, vehicle fuel and freshwater for Gaza Strip-Palestine,” *Fuel (Lond.)*, vol. 428, no. 140358, p. 140358, 2027.
[7] Y. Zhou, M. Zhou, R. Liu, B. Peng, S. Ye, and W. Huang, “Low-carbon steel production powered by photovoltaic-grid hybrid energy system: techno-economic and environmental assessment of integrated DRI-EAF configurations with different water electrolysis routes,” *Energy Convers. Manag.*, vol. 366, no. 121826, p. 121826, 2026.
[8] Y. Zhao, S. Zhang, J. Wei, and G. Li, “Low-carbon transition evaluation of park integrated energy systems incorporating hybrid energy storage systems and industrial by-product hydrogen,” *J. Energy Storage*, vol. 164, no. 122250, p. 122250, 2026.
[9] I. Imbayah, M. Hasan, H. El-Khozondare, M. Khaleel, A. Alsharif, and A. Ahmed, “Review paper on green hydrogen production, storage, and utilization techniques in Libya,” *jsesd*, vol. 13, no. 1, pp. 1–21, 2024.
[10] M. Khaleel *et al.*, “An optimization approaches and control strategies of hydrogen fuel cell systems in EDG-integration based on DVR technology,” *J. Eur. Syst. Autom.*, vol. 57, no. 2, pp. 551–565, 2024.
[11] M. Al-Mandhari, L. Morton, S. N. Hussain, Z. Zhou, Z. J. Chew, and A. Ghosh, “Floating photovoltaic-powered green hydrogen for decarbonization of the energy-consuming sectors in the United Kingdom,” *Energies*, vol. 19, no. 12, p. 2931, 2026.
[12] S. Rekik, I. Khabbouchi, D. Lounissi, M. Khaleel, D. Richards, and L. Kolsi, “Opportunities and challenges of solar-wind-powered hydrogen in emerging economies: A spatial and techno-economic analysis,” in *2025 Global Conference on Sustainable Energy and Net-Zero Emissions (SENZE)*, 2025, pp. 1–6.
[13] M. Mohamad and A. Hesri, “Hydrogen storage methods: Opportunities, safety, risk, and compliance assessment,” *ijees*, vol. 3, no. 4, pp. 17–32, 2025.
[14] S. Abulifa, M. M. Abubakr, and A. Alharam, “Hydrogen storage technologies: Current status, challenges, and future prospects,” *ijees*, vol. 4, no. 1, pp. 48–62, 2026.
[15] A. Alkhair and G. A. M. Ghalboun, “Environmental impacts on energy storage systems integrated with renewables,” *ijees*, vol. 4, no. 1, pp. 15–31, 2026.
[16] F. E. Abukhres, A. Algaddaf, and M. Ouadi, “Investigation and development the modelling of intermediate temperature PEM fuel cell for transport applications,” *ijees*, vol. 3, no. 1, pp. 61–82, 2025.
[17] S. Yamaguchi, H. Watanabe, R. Gotoda, C. N. Bonacina, and T. Kono, “Year-long demonstration of green hydrogen supply chain with portable and fast-charging metal hydride tanks,” *Int. J. Hydrogen Energy*, vol. 229, no. 154623, p. 154623, 2026.
[18] I. Bekki, F. E. Al Azhari, M. Kerrou, A. Afkari, and A. Oumachtaq, “Integral sliding mode control-based voltage regulation of a photovoltaic-powered microbial electrolysis cell for enhanced biohydrogen production,” *Transformative Energy*, vol. 3, no. 100022, p. 100022, 2026.
[19] I. Imbayah, O. A. Eseid, M. M. Beiek, K. Akter, A. Alsharif, and A. Ali Ahmed, “Recent developments in EV charging infrastructure: Opportunities and IoE framework challenges,” *ijees*, vol. 1, no. 4, pp. 47–63, 2023.
[20] M. Khaleel, Z. Yusupov, and W. A. Shah, “Artificial intelligence utilization for PQ concerns in power grid: Cybersecurity, optimization and policy implications,” in *2026 IEEE 5th International Maghreb Meeting of the Conference on Sciences and Techniques of Automatic Control and Computer Engineering (MI-STA)*, 2026, pp. 1–6.
[21] W. A. Shah, M. Khaleel, and J. Muhammad, “Improved voltage signal analysis and peak detection using AMPD for enhanced power grid efficiency,” in *2025 International Conference on Smart Grid and Energy (ICSGE)*, 2025, pp. 67–73.
[22] N. S. Hassan *et al.*, “Recent review and evaluation of green hydrogen production via water electrolysis for a sustainable and clean energy society,” *Int. J. Hydrogen Energy*, vol. 52, pp. 420–441, 2024.
[23] A. Serik, Z. Kuspanov, and C. Daulbayev, “Cost-effective strategies and technologies for green hydrogen production,” *Renew. Sustain. Energy Rev.*, vol. 226, no. 116242, p. 116242, 2026.

[24] M. Khaleel, Z. Yusupov, and W. A. Shah, “Towards electrolyser deployment and manufacturing capacity of China: Technological innovation, localization, investment, and policy,” in *2026 IEEE 5th International Maghreb Meeting of the Conference on Sciences and Techniques of Automatic Control and Computer Engineering (MI-STA)*, 2026, pp. 834–839.

[25] S. E. Hosseini and M. A. Wahid, “Hydrogen production from renewable and sustainable energy resources: Promising green energy carrier for clean development,” *Renew. Sustain. Energy Rev.*, vol. 57, pp. 850–866, 2016.

[26] M. Khaleel, Z. Yusupov, O. M. Bshina, M. M. Dali, and W. A. Shah, “Toward renewable energy deployment in North African countries: Potential resources, investments, transition scenario, opportunities, challenges, and policy,” *Unconventional Resources*, vol. 12, no. 100363, p. 100363, 2026.

[27] C. Anand *et al.*, “Green hydrogen for a sustainable future: A review of production methods, innovations, and applications,” *Int. J. Hydrogen Energy*, vol. 111, pp. 319–341, 2025.

[28] S. Al-Hashmi *et al.*, “Toward a sustainable energy future in the Gulf region: Overcoming barriers and enhancing renewable energy strategies,” *Energy Sources Part B: Econ. Plan. Policy*, vol. 21, no. 1, 2026.

[29] L. A. Swagatika Priyadarshini, V. Kaushik, and R. Kataria, “The role of anthropogenic activities, energy demand, and global climate change,” in *Advances in Geographical and Environmental Sciences*, Singapore: Springer Nature Singapore, 2025, pp. 35–61.

[30] C. W. Su, X. Y. Song, J. Dou, and M. Qin, “Fossil fuels or renewable energy? The dilemma of climate policy choices,” *Renew. Energy*, vol. 238, no. 121950, p. 121950, 2025.

[31] Y. Miao, A. A. Ather Bukhari, W. A. A. Bukhari, S. Ahmad, and N. Hayat, “Why fossil fuels stifle green economic growth? An environmental management perspective in assessing the spatial spillover impact of energy consumption in South Asia,” *J. Environ. Manage.*, vol. 373, no. 123471, p. 123471, 2025.

[32] B. Ju *et al.*, “Mapping regional disparities in the global shift toward decarbonized power systems,” *Carb Neutrality*, vol. 4, no. 1, 2025.

[33] M. Khaleel, E. Yaghoubi, E. Yaghoubi, and M. Z. Jahromi, “The role of mechanical energy storage systems based on artificial intelligence techniques in future sustainable energy systems,” *ijees*, vol. 1, no. 4, pp. 01–31, 2023.

[34] M. Khaleel, I. Imbayah, Y. Nassar, and H. J. El-Khozondar, “Renewable energy transition pathways and net-zero strategies,” *ijees*, vol. 3, no. 4, pp. 01–16, 2025.

[35] O. S. Abualoyoun and A. A. Amar, “Toward achieving net-zero in the evolution of the global energy sector,” *ijees*, vol. 3, no. 1, pp. 143–156, 2025.

[36] Y. Nassar *et al.*, “Solar and wind atlas for Libya,” *ijees*, vol. 1, no. 3, pp. 27–43, 2023.

[37] A. Alsharif *et al.*, “Applications of solar energy technologies in north Africa: Current practices and future prospects,” *ijees*, vol. 1, no. 3, pp. 164–173, 2023.

[38] K. M. Omemen and M. O. Aldbbah, “Climate change: Key contributors and sustainable solutions,” *ijees*, vol. 3, no. 1, pp. 10–27, 2025.

[39] M. Khaleel and M. Elbar, “Exploring the rapid growth of solar photovoltaics in the European Union,” *ijees*, vol. 2, no. 1, pp. 61–68, 2024.

[40] A. Bekkouche, F. Benidir, A. Lekbir, A. M. Samatar, and S. Mekhilef, “Sustainable campus energy transition: Integrating hybrid renewables and green hydrogen for net-zero operations,” *Fuel (Lond.)*, vol. 410, no. 137859, p. 137859, 2026.

[41] I. S. Sadkin, O. V. Borush, and P. A. Shchinnikov, “Analysis of energy consumption for auxiliaries of zero emissions sCO2 power plants,” *Energy Convers. Manag.*, vol. 323, no. 119266, p. 119266, 2025.

[42] A. Ashraf and M. Sagheer, “Renewable energy capacity and technological innovations: A review of global trends and future directions,” *Environ. Prog. Sustain. Energy*, vol. 44, no. 6, 2025.

[43] P. Achakulwisut, P. Erickson, C. Guivarch, R. Schaeffer, E. Brutschin, and S. Pye, “Global fossil fuel reduction pathways under different climate mitigation strategies and ambitions,” *Nat. Commun.*, vol. 14, no. 1, p. 5425, 2023.

[44] M. Almansuri, Z. Yusupov, and M. Khaleel, “Emerging trends in solar PV performance enhancement: Cooling, concentration, spectral splitting, and tracking techniques,” *ijees*, vol. 4, no. 1, pp. 32–47, 2026.

[45] H. S. Salem, M. Y. Pudza, and Y. Yihdego, “Harnessing the energy transition from total dependence on fossil to renewable energy in the Arabian Gulf region, considering population,

climate change impacts, ecological and carbon footprints, and United Nations' Sustainable Development Goals," *Sustain Earth Reviews*, vol. 6, no. 1, 2023.

[46] B. Gajdzik, R. Wolniak, R. Nagaj, B. Žuromskaitė-Nagaj, and W. W. Grebski, "The influence of the global energy crisis on energy efficiency: A comprehensive analysis," *Energies*, vol. 17, no. 4, p. 947, 2024.

[47] Y. F. Nassar *et al.*, "Carbon footprint and energy life cycle assessment of wind energy industry in Libya," *Energy Convers. Manag.*, vol. 300, no. 117846, p. 117846, 2024.

[48] Y. F. Nassar *et al.*, "Assessing the viability of solar and wind energy technologies in semi-arid and arid regions: A case study of Libya's climatic conditions," *Appl. Sol. Energy*, vol. 60, no. 1, pp. 149–170, 2024.

[49] A. M. Makhzom *et al.*, "Carbon dioxide Life Cycle Assessment of the energy industry sector in Libya: A case study," *ijees*, vol. 1, no. 3, pp. 145–163, 2023.

[50] M. Khaleel, Z. Yusupov, A. Ahmed, A. Alsharif, Y. Nassar, and H. El-Khozondar, "Towards sustainable renewable energy," *Appl. Sol. Energy*, vol. 59, no. 4, pp. 557–567, 2023.

[51] H. J. El-Khozondar *et al.*, "Photovoltaic solar energy for street lighting: A case study at Kuwaiti roundabout, Gaza strip, Palestine," *Power Engineering and Engineering Thermophysics*, vol. 3, no. 2, pp. 77–91, 2024.

[52] M. Khaleel and Z. Yusupov, "Advancing sustainable energy transitions: Insights on finance, policy, infrastructure, and demand-side integration," *Unconventional Resources*, vol. 9, no. 100274, p. 100274, 2026.

[53] R. Wolniak and B. Skotnicka-Zasadzień, "Development of wind energy in EU countries as an alternative resource to fossil fuels in the years 2016–2022," *Resources*, vol. 12, no. 8, p. 96, 2023.

[54] S. C. Obiora, O. Bamisile, Y. Hu, D. U. Ozsahin, and H. Adun, "Assessing the decarbonization of electricity generation in major emitting countries by 2030 and 2050: Transition to a high share renewable energy mix," *Heliyon*, vol. 10, no. 8, p. e28770, 2024.

[55] C. Breyer *et al.*, "On the history and future of 100% renewable energy systems research," *IEEE Access*, vol. 10, pp. 78176–78218, 2022.

[56] O. A. Marzouk, "Expectations for the role of hydrogen and its derivatives in different sectors through analysis of the four energy scenarios: IEA-STEPS, IEA-NZE, IRENA-PES, and IRENA-1.5°C," *Energies*, vol. 17, no. 3, p. 646, 2024.

[57] A. Abduallah *et al.*, "Leveraging hydrogen for covering energy shortage in an electricity subgrid," *waujpas*, pp. 245–254, 2026.

[58] M. Khaleel, Z. Yusupov, A. Hesri, P. Odil, R. Jahongir, and I. Imbayah, "AI applications for power quality challenges in distribution systems: Technical barriers and emerging trends," in *2026 IEEE 5th International Maghreb Meeting of the Conference on Sciences and Techniques of Automatic Control and Computer Engineering (MI-STA)*, 2026, pp. 846–851.

[59] D.-W. Li, J.-L. Huang, D. Yu, D. Zhang, and X.-L. Zhang, "Development of low-carbon technologies in China's integrated hydrogen supply and power system," *Adv. Clim. Chang. Res.*, vol. 15, no. 5, pp. 936–947, 2024.

[60] M. Ammar, B. O. Oyewale, A. Elseragy, I. M. Albayati, and A. M. Aliyu, "A global review of blue and green hydrogen fuel production technologies, trends and future outlook to 2050," *Fuels*, vol. 6, no. 4, p. 88, 2025.

[61] A. Boretti and B. G. Pollet, "Hydrogen economy: Paving the path to a sustainable, low-carbon future," *Int. J. Hydrogen Energy*, vol. 93, pp. 307–319, 2024.

[62] S. Dermühl and U. Riedel, "A comparison of the most promising low-carbon hydrogen production technologies," *Fuel (Lond.)*, vol. 340, no. 127478, p. 127478, 2023.

[63] B. Li, X. Hu, Y. Li, J. He, and Z. Wu, "Coordinated operation optimization of an off-grid PV–PEM hydrogen production system considering efficiency and lifetime," *Int. J. Hydrogen Energy*, vol. 256, no. 156067, p. 156067, 2026.

[64] Y. Zhang *et al.*, "Prediction of breakthrough time in hydrogen purification from coke oven gas using deep learning model," *J. Clean. Prod.*, vol. 574, no. 149003, p. 149003, 2026.

[65] P. A. Nikrityuk, "Hydrogen economy and engineering: A new cross-border journal connecting the new hydrogen economy and science & engineering," *Hydrogen Economy & Engineering*, vol. 1, no. 100001, p. 100001, 2026.

[66] B. S. Zainal *et al.*, "Recent advancement and assessment of green hydrogen production technologies," *Renew. Sustain. Energy Rev.*, vol. 189, no. 113941, p. 113941, 2024.

[67] P. Fernández-Arias, Á. Antón-Sancho, G. Lampropoulos, and D. Vergara, “On green hydrogen generation technologies: A bibliometric review,” *Appl. Sci. (Basel)*, vol. 14, no. 6, p. 2524, 2024.

[68] N. Sazali, “Emerging technologies by hydrogen: A review,” *Int. J. Hydrogen Energy*, vol. 45, no. 38, pp. 18753–18771, 2020.

[69] M. Khaleel *et al.*, “Battery technologies In electrical power Systems: Pioneering secure energy transitions,” *J. Power Sources*, vol. 653, no. 237709, p. 237709, 2025.

[70] A. Alsharif, C. W. Tan, R. Ayop, A. Ali Ahmed, M. Mohamed Khaleel, and A. K. Abobaker, “Power management and sizing optimization for hybrid grid-dependent system considering photovoltaic wind battery electric vehicle,” in *2022 IEEE 2nd International Maghreb Meeting of the Conference on Sciences and Techniques of Automatic Control and Computer Engineering (MI-STA)*, 2022.

[71] M. Khaleel, Z. Yusupov, N. Yasser, H. Elkhozondar, and A. A. Ahmed, “An integrated PV farm to the unified power flow controller for electrical power system stability,” *ijees*, vol. 1, no. 1, pp. 18–30, 2023.

[72] A. Ghayth, Z. Yusupov, A. Hesri, and M. Khaleel, “Performance enhancement of PV array utilizing Perturb & Observe algorithm,” *ijees*, vol. 1, no. 2, pp. 29–37, 2023.

[73] Mohamed M. Abubaker, “Investment Pathways for Renewable Energy: Opportunities, Challenges and Policy Directions”, *ljsdr*, vol. 2, no. 2, pp. 1–21, Jul.

[74] Saleh A. Emhanna and Ramzi S. Salem, “A Geological Screening Framework for Underground Green Hydrogen Storage in Libya: Basin-Scale Evaluation and Site Prioritization”, *ljsdr*, vol. 2, no. 2, pp. 70–83, Jul. 2026, Accessed: Aug. 03, 2026.

[75] Muftah Ali and Mohamed Khaleel, “Decarbonizing Buildings at Scale: Energy Codes, Innovation Pathways, and the Net-Zero Transition”, *ljsdr*, vol. 1, no. 1, pp. 45–51, Dec. 2025, Accessed: Aug. 03, 2026.

[76] Mohamed Khaleel and Ali Hesri, “Improving Power System Reliability Using Hydrogen Fuel Cell–Integrated D-FACTS for Power Quality Enhancement”, *ljsdr*, vol. 1, no. 1, pp. 01–16, Nov. 2025,